AKR1B1 promotes basal-like breast cancer progression by a positive feedback loop that activates the EMT program

Xuebiao Wu,[1,2]* Xiaoli Li,[1,2]* Qiang Fu,[4]* Qianhua Cao,[1,2] Xingyu Chen,[1,2] Mengjie Wang,[1,2] Jie Yu,[1,2] Jingpei Long,[3] Jun Yao,[5] Huixin Liu,[1,2] Danping Wang,[1,2] Ruocen Liao,[1,2] and Chenfang Dong[1,2]

[1]Department of Pathology and Pathophysiology, [2]Zhejiang Key Laboratory for Disease Proteomics, and [3]Department of Breast Surgery, Women's Hospital, Zhejiang University School of Medicine, Hangzhou 310058, China
[4]Department of Immunology, Binzhou Medical University, Yantai 264003, China
[5]Department of Neuro-oncology, M.D. Anderson Cancer Center, The University of Texas, Houston, TX 77030

Basal-like breast cancer (BLBC) is associated with high-grade, distant metastasis and poor prognosis. Elucidating the determinants of aggressiveness in BLBC may facilitate the development of novel interventions for this challenging disease. In this study, we show that aldo-keto reductase 1 member B1 (AKR1B1) overexpression highly correlates with BLBC and predicts poor prognosis in breast cancer patients. Mechanistically, Twist2 transcriptionally induces AKR1B1 expression, leading to nuclear factor κB (NF-κB) activation. In turn, NF-κB up-regulates Twist2 expression, thereby fulfilling a positive feedback loop that activates the epithelial–mesenchymal transition program and enhances cancer stem cell (CSC)–like properties in BLBC. AKR1B1 expression promotes, whereas AKR1B1 knockdown inhibits, tumorigenicity and metastasis. Importantly, epalrestat, an AKR1B1 inhibitor that has been approved for the treatment of diabetic complications, significantly suppresses CSC properties, tumorigenicity, and metastasis of BLBC cells. Together, our study identifies AKR1B1 as a key modulator of tumor aggressiveness and suggests that pharmacologic inhibition of AKR1B1 has the potential to become a valuable therapeutic strategy for BLBC.

INTRODUCTION

Breast cancer is a heterogeneous disease with four major subtypes according to gene expression profiling: luminal A, luminal B, HER2, and basal like (Vargo-Gogola and Rosen, 2007). Compared with the other subtypes, basal-like breast cancer (BLBC) is associated with an aggressive clinical history, early recurrence, distant metastasis, and shorter survival (Kreike et al., 2007; Rakha et al., 2008). BLBC usually occurs in younger and premenopausal women and has a tendency toward early metastatic spread to the brain and lungs, sites known to be associated with a poor prognosis (Blick et al., 2008; Sarrió et al., 2008; Storci et al., 2008; Bergamaschi et al., 2009; Hennessy et al., 2009). A lack of effective targeted therapies for BLBC often results in a rapidly fatal clinical outcome. An important prerequisite for targeted therapies is to understand the molecular mechanisms underlying the metastatic process associated with BLBC. Notably, BLBC possesses the activated epithelial–mesenchymal transition (EMT) program, which is required for tumor progression and metastasis (Mani et al., 2008; Gupta et al., 2009; Polyak and Weinberg, 2009; Valastyan and Weinberg, 2011; Dong et al., 2013b).

EMT is a phenotypic conversion that facilitates embryonic development, wound healing, and cancer metastasis (Polyak and Weinberg, 2009; Valastyan and Weinberg, 2011; Dong et al., 2012; Ye and Weinberg, 2015). During EMT, epithelial cells lose their epithelial properties and acquire a motile mesenchymal phenotype (Polyak and Weinberg, 2009; Ye and Weinberg, 2015). Importantly, EMT causes the acquisition of cancer stem cell (CSC)–like properties (Mani et al., 2008; Gupta et al., 2009; Valastyan and Weinberg, 2011; Liu et al., 2015). As tumor cells that have undergone EMT often faced a harsh environment of foreign tissue during the metastatic process, they must rewire metabolic and oncogenic pathways to meet the demands of survival and metastasis. Characterization of the causal relationship between EMT and metabolic alteration will help to develop novel interventions for targeting metastatic breast cancer.

Metabolic reprograming has been accepted as a hallmark of cancer (Hanahan and Weinberg, 2011). Lipid metabolism, which represents an important source of bioactive molecules, is implicated in tumor progression (Tammali et al., 2011; Carracedo et al., 2013). Arachidonic acid (AA) is a polyunsaturated fatty acid that is metabolized into prostaglandins (PGs), hydroperoxyeicosatetraenoic acids, and epoxyeicosatrienoic acids through a series of enzyme-catalyzed reactions (Brash, 2001). AA-related enzymes and their metabolites are involved

*X. Wu, X. Li, and Q. Fu contributed equally to this paper.

Correspondence to Chenfang Dong: chenfangdong@zju.edu.cn

Abbreviations used: AA, arachidonic acid; AKR1, aldo-keto reductase 1; BLBC, basal-like breast cancer; ChIP, chromatin immunoprecipitation; CSC, cancer stem cell; EMT, epithelial–mesenchymal transition; NADPH, nicotinamide adenine dinucleotide phosphate reduced; PG, prostaglandin; ROS, reactive oxygen species; TSS, transcription start site.

The Rockefeller University Press $30.00
J. Exp. Med. 2017 Vol. 214 No. 4 1065–1079
https://doi.org/10.1084/jem.20160903

in pathophysiological processes of many diseases, including a variety of cancers (Brash, 2001; Tammali et al., 2011). Aldo-keto reductase 1 member B1 (AKR1B1), which catalyzes the reduction of PGH2 to PGF2α, is a major nicotinamide adenine dinucleotide phosphate reduced (NADPH)–dependent PGF synthase during AA metabolism. PGF2α, a major metabolite of AKR1B1, modulates cell adhesion, migration, and invasion via PGF2α receptor–mediated signaling in endometrial cancer (Sales et al., 2008), suggesting that AKR1B1 may be involved in tumor progression by modulating lipid metabolism. While investigating Twist2-mediated induction of EMT in BLBC, we unexpectedly identified that AKR1B1 expression is elevated by Twist2. AKR1B1 expression provides tumorigenic and metastatic advantage in BLBC through a positive regulatory feedback loop that activates the EMT program and enhances stem cell–like properties. Our study not only reveals a critical mechanism of how AKR1B1 contributes to EMT and metastasis, but also provides a potential target for the treatment of BLBC.

RESULTS

AKR1B1 is enriched in the BLBC subtype

We recently showed that loss of fructose-1,6-biphosphatase (FBP1) by Snail-mediated repression provided metabolic advantages in BLBC (Dong et al., 2013b). To systematically identify other metabolic genes required for BLBC, we analyzed gene expression profiles of various subtypes of breast cancer in two publicly available cDNA microarray datasets (GEO accession no. GSE25066 and dataset NKI295), which contain 508 and 295 breast cancer patients, respectively (van de Vijver et al., 2002; Hatzis et al., 2011). Several known genes previously shown to have important roles in BLBC were observed to have significant differences between BLBC and other subtypes, such as *lactate dehydrogenase B* (*LDHB*) and *FBP1*. Notably, *AKR1B1* expression was significantly higher in BLBC than in other subtypes, whereas expressions of other PGH2 reductases such as *AKR1C3* and *FAM213B* did not have obvious changes in different subtypes (Fig. 1 A and Fig. S1 A). To confirm this finding, we collected fresh frozen breast tumor tissues from 9 cases of luminal and 21 cases of triple-negative breast cancer (triple-negative in the expression of ERα, PR, and HER2/neu; sometimes used as a surrogate term for basal like). Consistently, the expressions of AKR1B1 and Twist2 were elevated in triple-negative breast cancer, and their expressions were significantly down-regulated in the luminal subtype of breast cancers (Fig. 1 B and Fig. S1 B). To further extend these observations, we also analyzed *AKR1B1* expression in another four gene expression datasets (GEO accession nos. GSE12777, GSE10890, and GSE16732; and ArrayExpress accession no. E-TABM-157), which contain 51, 52, 41, and 51 breast cancer cell lines, respectively (Neve et al., 2006; Hoeflich et al., 2009; Riaz et al., 2009). Similar to the observations in the GSE25066 and NKI295 datasets and in breast cancer tissues, *AKR1B1* overexpression correlated with basal subtype of breast cancer cell lines (Fig. 1 C). Then, we confirmed these findings by either semiquantitative RT-PCR or quantitative real-time PCR in a representative panel of breast cancer cell lines that contained five luminal and five BLBC cell lines. Consistently, *AKR1B1* mRNA expression was remarkably elevated in five BLBC cell lines (Fig. 1, D and E). We further examined the protein levels of AKR1B1 and EMT markers in these cell lines. BLBC cell lines lost the expression of epithelial molecule (E-cadherin) and contained high levels of mesenchymal markers (vimentin, N-cadherin, and Twist2). Importantly, AKR1B1 protein level also was high in BLBC cell lines, whereas it was absent in luminal cell lines (Fig. 1 F). Together, our data indicate that AKR1B1 overexpression is correlated with BLBC, underscoring the importance of characterizing potential function and mechanism of AKR1B1 for this subtype of breast cancer.

AKR1B1 is a direct target of Twist2

When investigating the correlation between AKR1B1 and BLBC, AKR1B1 and Twist2 displayed similar expression patterns in breast cancer cell lines and tissues (Fig. 1, B and F). When *AKR1B1* expression was plotted against *Twist2* expression in two microarray datasets (GSE10890 and GSE12777) that contain 52 and 51 breast cancer cell lines, respectively (Hoeflich et al., 2009), *AKR1B1* expression positively correlated with *Twist2* expression in both datasets (Fig. 2 A). A similar result was obtained in a dataset from The Cancer Genome Atlas (TCGA; 1,215-patient samples; Fig. S2 A). The positive correlation between AKR1B1 and Twist2 in breast cancer prompted us to investigate their mutually causal relationships. To this end, we established stable clones with empty vector or Twist2 expression in T47D cells. As anticipated, Twist2 expression substantially down-regulated E-cadherin expression and induced a morphological change indicative of EMT in T47D cells (Fig. 2 B). Intriguingly, Twist2 but not Twist1, Snail, or Slug expression remarkably promoted AKR1B1 expression in T47D cells (Fig. 2, B and C; and Fig. S2 B). Similar results were obtained in MCF7 cells with exogenous Twist2 expression (Fig. 2 C). We also generated stable transfectants with empty vector or knockdown of Twist2 expression in two BLBC cell lines (MDA-MB231 and SUM159). Strikingly, knockdown of Twist2 expression restored E-cadherin expression and down-regulated AKR1B1 expression (Fig. 2 C). These data suggest that Twist2 as a transcriptional factor may induce AKR1B1 expression via transcriptional regulation.

Given the immediate induction of AKR1B1 by Twist2 and their mutual correlation in breast cancer cell lines and tissues, we sought to determine whether AKR1B1 expression is regulated directly by Twist2. A survey of a DNA sequence in the AKR1B1 locus revealed that the proximal AKR1B1 promoter contains seven potential Twist2-binding E-boxes (CANNTG) from −1374 bp to the transcription start site (TSS; Fig. S2 C). To determine whether these E-boxes are crucial for Twist2-mediated gene transcription, we cloned the human AKR1B1 promoter and generated several dele-

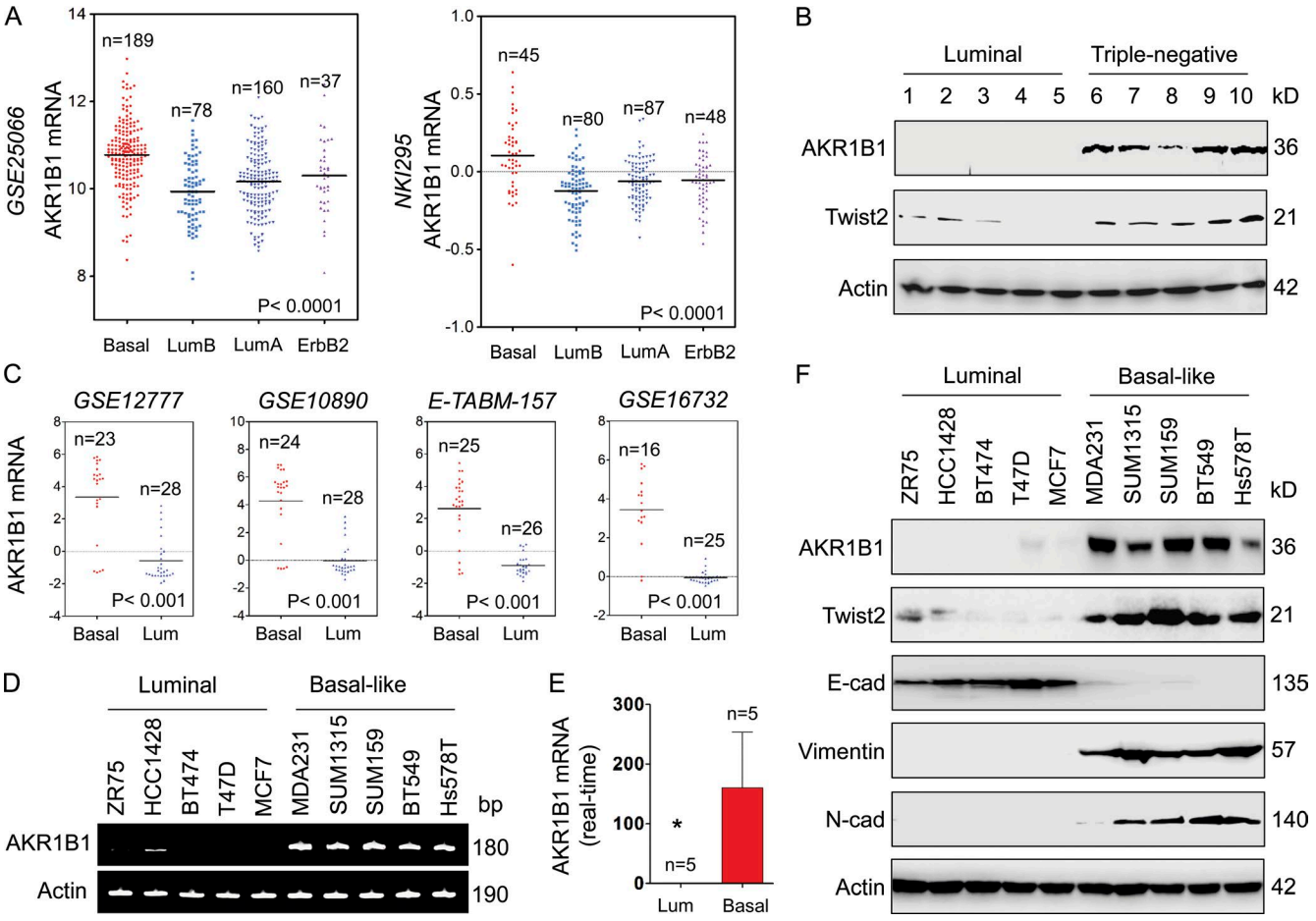

Figure 1. **AKR1B1 overexpression highly correlates with BLBC.** (A) Dot plots indicate *AKR1B1* expression in different subtypes of breast cancer from microarray datasets (GSE25066 and NKI295). Comparisons were analyzed by one-way ANOVA. (B) Expression of AKR1B1 and Twist2 was analyzed by Western blotting in fresh frozen tumor samples from five cases of luminal and five cases of triple-negative breast cancer (other analyses of 20 cases of fresh tumor samples are shown in Fig. S1 B). (C) Dot plots indicate *AKR1B1* expression in luminal and BLBC cell lines from four microarray datasets (GSE12777, GSE10890, GSE16732, and E-TABM-157). Comparisons were made using two-tailed Student's *t* test. (D and E) Expression of *AKR1B1* mRNA was examined by either semiquantitative RT-PCR (D) or quantitative real-time PCR (E) in a representative panel of breast cancer cell lines. Data are mean ± SD. *, $P < 0.05$ by Student's *t* test. (F) Expression of AKR1B1, Twist2, E-cadherin, and other EMT markers in cells from D was analyzed by Western blotting. E-cad, E-cadherin; Lum, luminal; N-cad, N-cadherin.

tion mutants of promoter–luciferase constructs based on the location of these E-boxes, including wtA (−1,374 bp), wtA1 (−1,020 bp), and wtA2 (−583 bp; Fig. S2 C). By expressing the wtA in T47D, MCF7, MDA-MB231, and SUM159 cells, Twist2 significantly promoted AKR1B1 promoter luciferase activity (Fig. 2 E). The wtA1 without the region between −1,374 and −1,021 bp still maintained high reporter activity induced by Twist2 (wtA vs. wtA1), whereas the wtA2 (−583 bp) lost the activity to respond to Twist2 expression (Fig. S2 C). Thus, the region between −1,020 and −584 bp might be important for Twist2-mediated AKR1B1 activation. To pinpoint the exact binding E-boxes, we introduced point mutations into E1 and/or E2. Mutation in E1 (mutA1) did not significantly reduce, whereas mutation in either E2 (mutA2) or both E-boxes (mutA3) almost completely abolished, Twist2-mediated activation of the AKR1B1 promoter luciferase (Fig. 2 F), suggesting that Twist2 activates the AKR1B1 promoter in an E-box–dependent fashion and that the E-box at −997 bp is required for Twist2-induced transcriptional activation. We also performed chromatin immunoprecipitation (ChIP) assay after wtA1 as well as its E-box mutants (mutA1, mutA2, and mutA3) were coexpressed with empty vector or Twist2 in HEK293 cells. As expected, mutation in either E2 (mutA2) or both E-boxes (mutA3) dramatically attenuated the binding of Twist2 to the AKR1B1 promoter, indicating the E-box at −997 bp is a critical Twist2-binding site (Fig. S2 D). Furthermore, we revealed that Twist2 directly bound to the AKR1B1 promoter in MDA-MB231 and SUM159 cells by ChIP assay (Fig. 2 G). These data indicate that AKR1B1 is a direct target of Twist2.

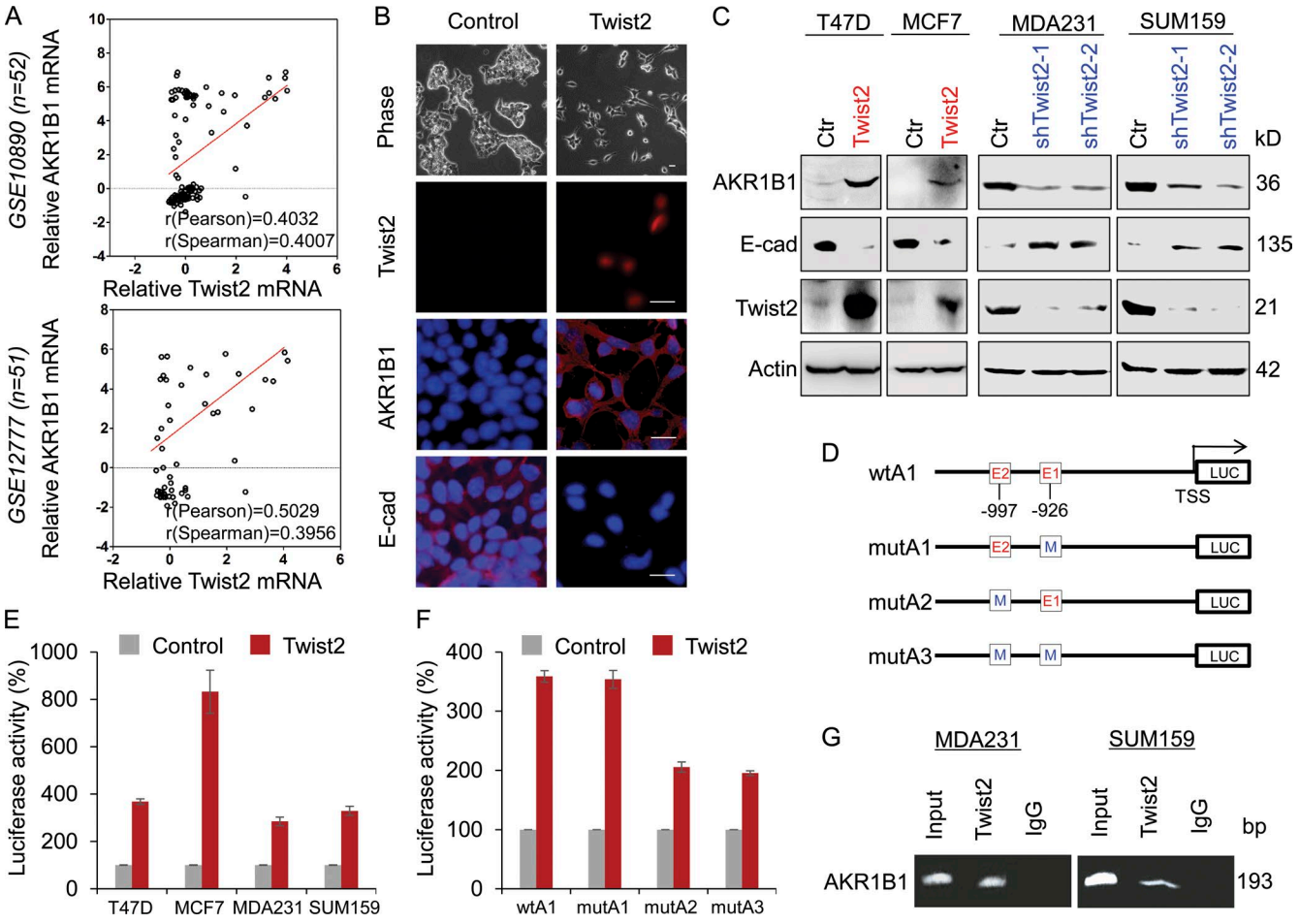

Figure 2. **AKR1B1 positively correlates with Twist2 expression and is a direct transcriptional target of Twist2.** (A) Analysis of public datasets (GSE10890 and GSE12777) for the expression of *AKR1B1* and *Twist2*. The relative level of AKR1B1 was plotted against that of Twist2. Correlations were analyzed using Pearson's correlation method and Spearman's rank correlation test. (B) Stable clones with empty vector or Twist2 expression were established in T47D cells. Morphological changes indicative of EMT are shown in the phase contrast images. Expression of AKR1B1, E-cadherin (E-cad), and Twist2 was analyzed by immunofluorescent staining. Nuclei were visualized with DAPI (blue). Bar, 20 µm. (C) Expression of AKR1B1, E-cadherin, and Twist2 was analyzed by Western blotting in T47D and MCF7 cells infected with empty vector (Ctr) or Twist2-expressing vector (left), as well as MDA-MB231 and SUM159 cells with stable empty vector or knockdown of Twist2 expression (right). (D) Schematic diagram showing positions of potential Twist2-binding E-boxes in AKR1B1 promoter and AKR1B1 promoter luciferase (LUC) constructs used. E, E-box; M, mutated. (E) AKR1B1 promoter luciferase construct (wtA) was coexpressed with empty vector or Twist2 in T47D, MCF7, MDA-MB231, and SUM159 cells, respectively. After 48 h, luciferase activities were determined and normalized (mean ± SD in three separate experiments). (F) AKR1B1 promoter luciferase construct (wtA1) as well as its E-box mutants (mutA1, mutA2, and mutA3) were coexpressed with empty vector or Twist2 in T47D cells. Luciferase activities were determined and normalized as in E. (G) ChIP analysis for binding of Twist2 to the AKR1B1 promoter in MDA-MB231 and SUM159 cells.

AKR1B1 alters the expression of EMT markers and enhances breast cancer cell migration and invasion

To study the molecular function and mechanism of AKR1B1, we established stable transfectants with empty vector or knockdown of AKR1B1 expression in MDA-MB231 and SUM159 cells and clones with empty vector or AKR1B1 expression in T47D and MCF7 cells (Fig. 3, A and C). Because AKR1B1 is a direct transcriptional target of Twist2 that plays critical roles in EMT and tumor metastasis, we first examined whether AKR1B1 was associated with EMT in these cells. Indeed, knockdown of AKR1B1 expression significantly caused an increase in E-cadherin expression, whereas ectopic AKR1B1 expression reversed the up-regulation of E-cadherin in MDA-MB231 and SUM159 cells with stable knockdown of AKR1B expression (Fig. 3 A and Fig. S3 A). Epalrestat, a specific inhibitor of AKR1B1, also restored E-cadherin expression in MDA-MB231 and SUM159 cells (Fig. 3 B). Conversely, in AKR1B1-expressing cells, E-cadherin expression was greatly down-regulated (Fig. 3 C). To further establish the functional relationship of AKR1B1 and EMT, we measured the E-cadherin promoter luciferase activity. We observed that knockdown of AKR1B1 expression

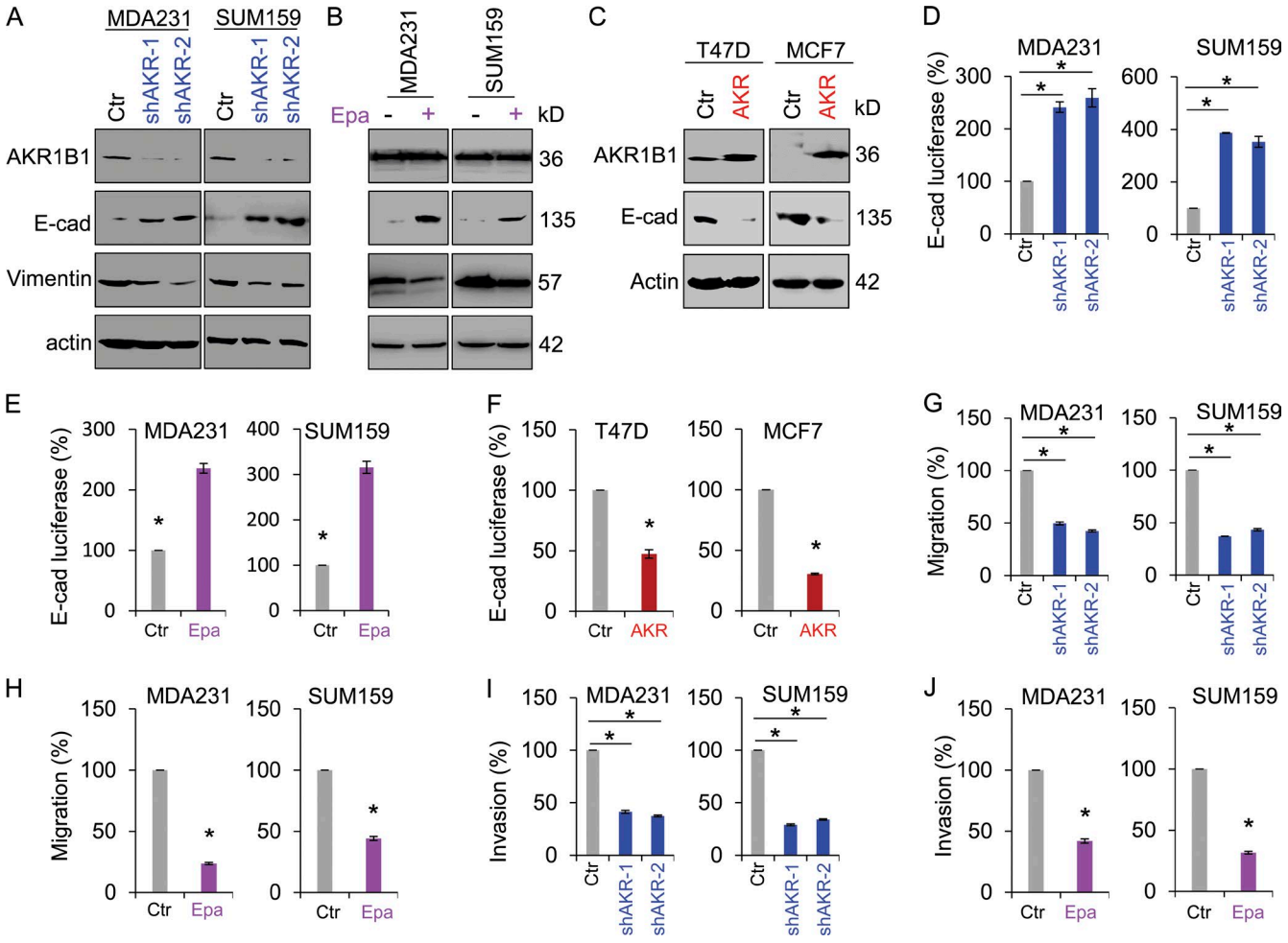

Figure 3. **AKR1B1 alters the expression of EMT markers and enhances breast cancer cell migration and invasion.** (A and B) Expression of AKR1B1, E-cadherin (E-cad), and vimentin was analyzed by Western blotting in MDA-MB231 and SUM159 cells with stable empty vector (Ctr) or knockdown of AKR1B1 expression (shAKR; A), as well as MDA-MB231 and SUM159 cells treated with or without 20 µM epalrestat (Epa; B). (C) Expression of AKR1B1 and E-cadherin was analyzed by Western blotting in T47D and MCF7 cells with stable empty vector or AKR1B1 expression (AKR). (D–F) E-cadherin reporter activity was measured in MDA-MB231 and SUM159 cells with stable empty vector or knockdown of AKR1B1 expression (D) and MDA-MB231 and SUM159 cells treated with or without 20 µM epalrestat (E), as well as T47D and MCF7 cells with stable empty vector or AKR1B1 expression (F). After 48 h, luciferase activities were normalized and determined. (G–J) Migratory ability (G and H) and invasiveness (I and J) of MDA-MB231 and SUM159 cells with stable empty vector or knockdown of AKR1B1 expression (G and I), as well as MDA-MB231 and SUM159 cells treated with or without 20 µM epalrestat (H and J), were analyzed. The percentage of migratory and invasive cells is shown in the bar graphs. Data are mean ± SD in three separate experiments. *, $P < 0.01$ by Student's *t* test.

or epalrestat reversed the suppression of the E-cadherin promoter in MDA-MB231 and SUM159 cells (Fig. 3, D and E; and Fig. S3 B), whereas AKR1B1 expression significantly decreased E-cadherin promoter luciferase activity in T47D and MCF7 cells (Fig. 3 F). Because suppression of E-cadherin can promote cell migration and invasion in the presence or absence of EMT (Onder et al., 2008) and because AKR1B1 is associated with suppression of E-cadherin, we hypothesized that AKR1B1 is critical for breast cancer cell migration and invasion. As expected, knockdown of AKR1B1 expression or epalrestat dramatically repressed the migration and invasion of MDA-MB231 and SUM159 cells in vitro (Fig. 3, G–J; and Fig. S3, C and D). Together, these observations indicate an important role for AKR1B1 in induction of EMT and acquisition of migratory and invasive ability in breast cancer cells.

AKR1B1 controls intracellular PGF2α levels and mediates the NF-κB pathway

To understand the metabolic consequence of AKR1B1 expression, we first measured the production of PGF2a, a major metabolite of AKR1B1 (Fig. 4 A). We noticed that knockdown of AKR1B1 expression or epalrestat significantly reduced PGF2a production in MDA-MB231 and SUM159 cells (Fig. 4 B and Fig. S4 A), whereas exogenous AKR1B1 expression increased PGF2a production in T47D and MCF7 cells (Fig. 4 C). These data indicate that AKR1B1 is required

for increased PGF2a production in breast cancer cells. We speculated that AKR1B1 might promote breast cancer cell migration and invasion via the PGF2α-mediated pathway. As anticipated, PGF2a markedly induced the migration and invasion of MDA-MB231 and SUM159 cells in vitro (Fig. 4, D and E). AKR1B1, a monomeric NADPH-dependent cytosolic enzyme, leads to a decrease in the ratio of NADPH/$NADP^+$ (Fig. 4 A). A decrease in the NADPH/$NADP^+$ ratio could cause oxidative stress (Kinoshita et al., 1981; Srivastava et al., 2005; Gloire et al., 2006). This is consistent with our findings that knockdown of AKR1B1 expression caused a significant decrease of reactive oxygen species (ROS) levels in MDA-MB231 cells, whereas ectopic AKR1B1 expression induced an obvious increase of ROS in T47D cells (Fig. S4 B). Because NF-κB is a redox-sensitive transcription factor that has been proposed to be the sensor for ROS (Li and Karin, 1999; D'Angio and Finkelstein, 2000; Gloire et al., 2006), AKR1B1-mediated increase of ROS may involve NF-κB signaling. Additionally, growing evidence also suggests that AKR1B1 can activate NF-κB signaling via the PGF2a-mediated pathway (Ramana et al., 2004; Tammali et al., 2006). Indeed, knockdown of AKR1B1 expression caused a dramatic decrease of RelA level, whereas AKR1B1 expression led to a marked increase of RelA expression in both the nucleus and cytoplasm (Fig. 4 F and Fig. S4 C). To further confirm the functional relationship between AKR1B1 and NF-κB, we measured NF-κB reporter luciferase. Strikingly, knockdown of AKR1B1 expression decreased the activity of NF-κB reporter in MDA-MB231 and SUM159 cells (Fig. 4 G), whereas AKR1B1 expression enhanced NF-κB promoter luciferase activity in T47D and MCF7 cells (Fig. 4 H).

RelA transcriptionally induces Twist2 expression

The NF-κB pathway has been implicated in the regulation of EMT (Huber et al., 2004; Zhou et al., 2004). To investigate the role of AKR1B1-mediated NF-κB signaling in EMT induction, we determined the expressions of RelA and various transcriptional factors of EMT by Western blotting. We observed that knockdown of AKR1B1 expression significantly decreased RelA and Twist2 expression but not Twist1, Snail, and Slug expression in MDA-MB231 and SUM159 cells, whereas AKR1B1 expression significantly increase RelA and Twist2 expression in T47D and MCF7 cells (Fig. 5 A). It is well known that TNF and IL-1β contribute to NF-κB activation. Indeed, RelA expression was induced by TNF or IL-1β in MDA-MB231 and SUM159 cells. Importantly, Twist2 expression also was dramatically up-regulated upon TNF or IL-1β stimulation in these cells (Fig. 5 B). These data suggest that Twist2 expression is positively correlated with RelA expression. To further investigate the relationship between RelA and Twist2, we established stable transfectants with empty vector or knockdown of RelA expression as well as stable clones with empty vector or RelA expression in MDA-MB231 and SUM159 cells. Strikingly, knockdown of RelA expression caused a decrease, whereas RelA expression resulted in an increase, in Twist2 expression (Fig. 5 C), indicating a critical role of RelA in regulating Twist2 expression.

To demonstrate whether Twist2 expression is regulated directly by RelA, four putative NF-κB–binding motifs were noticed in the proximal Twist2 promoter sequence from −222 bp to TSS (Fig. 5 D). We generated an AKR1B1 promoter–luciferase construct (wtT = TSS to −369 bp). By expressing the wtT in T47D, MDA-MB231, and HEK293 cells, a two- to fourfold increase in Twist2 promoter activity was observed in cells undergoing RelA overexpression (Fig. S4 D). To further define the elements inside the human Twist2 promoter that are involved in this activation, several point mutants were generated in the NF-κB–binding motifs (mutT1, mutT2, and mutT3; Fig. 5 D). Either the mutT1 or the mutT2, especially the latter, became less sensitive to, whereas the mutT3 with mutation of each NF-κB–binding motif almost completely lost, RelA-mediated activation of Twist2 promoter luciferase (Fig. 5 E), suggesting that all four of these consecutive NF-κB–binding motifs are important for RelA-mediated Twist2 activation. To further examine whether RelA directly binds to the Twist2 promoter, a ChIP assay was performed using MDA-MB231 and SUM159 cells. We detected a dramatic enrichment of RelA in the Twist2 promoter (Fig. 5 F). These data indicate that RelA up-regulates Twist2 expression by directly binding to the Twist2 promoter.

AKR1B1 contributes to the maintenance of CSCs and is required for tumorigenicity and metastasis of breast cancer

Many solid tumors contain a small population of highly tumorigenic CSCs, which contribute significantly to tumor initiation and metastasis. Emerging evidence has shown that the EMT program generates cells with stem cell–like properties (Polyak and Weinberg, 2009; Thiery et al., 2009; Nauseef and Henry, 2011). As AKR1B1 is highly expressed and involved in the EMT process in BLBC, we speculated that AKR1B1 expression might confer stem cell–like properties to BLBC cells. To test this notion, we examined tumorsphere formation of these cells. Strikingly, knockdown of AKR1B1 expression or epalrestat greatly suppressed tumorsphere formation in MDA-MB231 and SUM159 cells, whereas AKR1B1 expression in T47D cells enhanced tumorsphere formation (Fig. 6, A–C). As breast CSCs are enriched in cells with a $CD44^{high}/CD24^{low}$ phenotype (Fillmore and Kuperwasser, 2007; Blick et al., 2010), we then examined the potential effect of AKR1B1 on cell population with $CD44^{high}/CD24^{low}$ markers using flow cytometry analysis. Similar to the observation in tumorsphere formation, knockdown of AKR1B1 expression or epalrestat significantly reduced the percentage of $CD44^{high}/CD24^{low}$ population in MDA-MB231 and SUM159 cells, whereas AKR1B1 expression induced a remarkable increase of $CD44^{high}/CD24^{low}$ population in T47D cells (Fig. 6, D–H).

CSCs are highly tumorigenic and metastatic (Rosen and Jordan, 2009; Liu and Wicha, 2010; Badve and Nakshatri, 2012). First, we investigated AKR1B1's role in cell growth. Knockdown of AKR1B1 expression or epalrestat did not

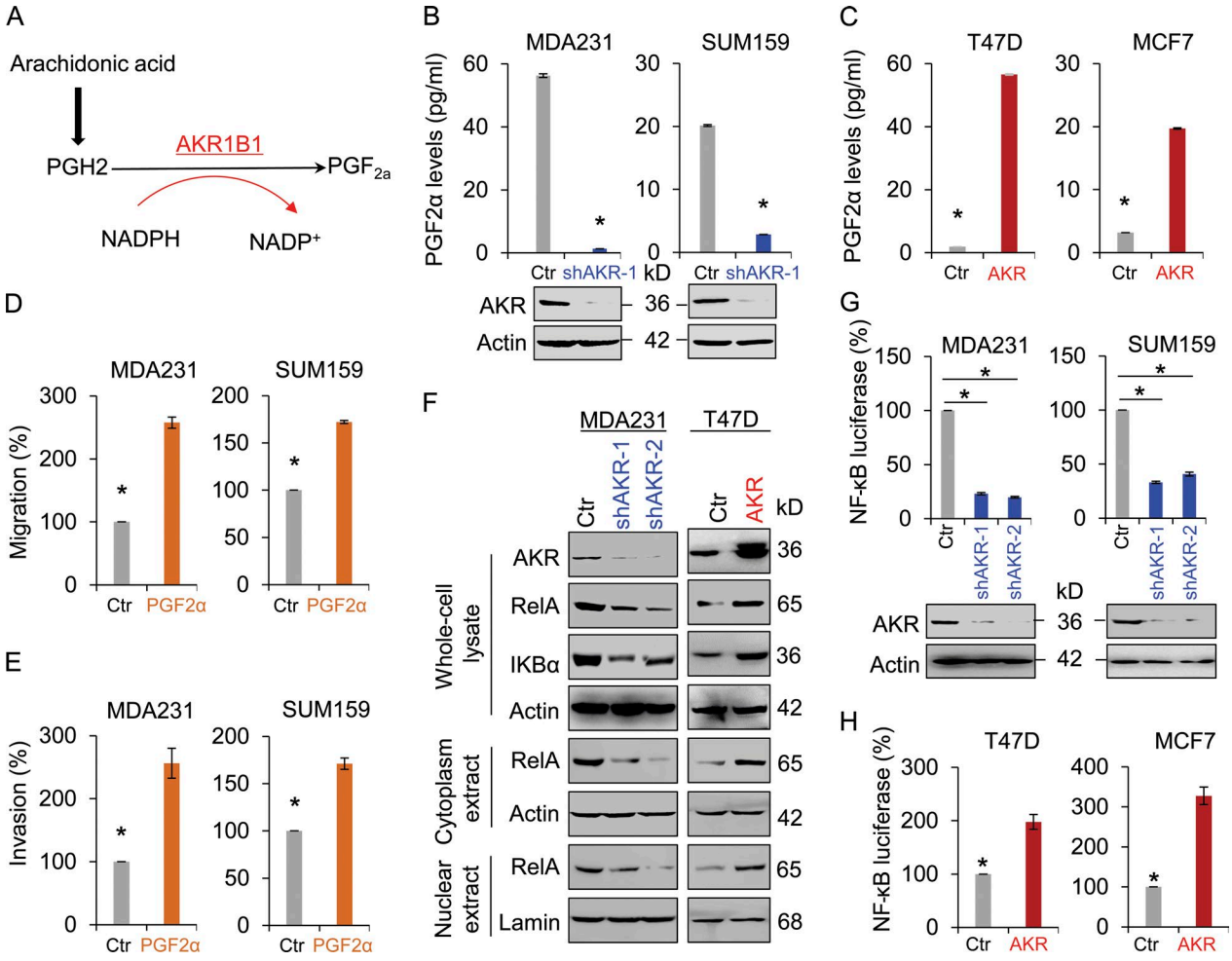

Figure 4. **AKR1B1 controls intracellular PGF2α levels and mediates the NF-κB pathway.** (A) PGF2α biosynthesis pathway. (B and C) The level of PGF2α was measured in MDA-MB231 and SUM159 cells with stable empty vector (Ctr) or knockdown of AKR1B1 expression (B), as well as T47D and MCF7 cells with stable empty vector or AKR1B1 expression (C). The level of PGF2α is shown in the bar graph. (D and E) Migratory ability (D) and invasiveness (E) of MDA-MB231 and SUM159 cells treated with or without 100 µM PGF2α were analyzed. The percentage of migratory and invasive cells is shown in the bar graph. (F) Expression of AKR1B1, RelA, and IKBα was analyzed by Western blotting in MDA-MB231 with stable empty vector or knockdown of AKR1B1 expression (left), as well as T47D cells with stable empty vector or AKR1B1 expression (right). (G and H) NF-κB reporter activity was examined in MDA-MB231 and SUM159 cells with stable empty vector or knockdown of AKR1B1 expression (G), as well as T47D and MCF7 cells with stable empty vector or AKR1B1 expression (H). After 48 h, luciferase activities were normalized and determined. Data are mean ± SD in three separate experiments. *, $P < 0.01$ by Student's *t* test.

cause an apparent effect on the growth of MDA-MB231 and SUM159 cells (Fig. S5, A and B). Then, we examined the effect of AKR1B1 expression on the in vitro tumorigenicity using soft agar assay. Knockdown of AKR1B1 expression or epalrestat caused a dramatic decrease of colonies in MDA-MB231 and SUM159 cells, whereas AKR1B1 expression led to a marked increase of colony formation in T47D cells (Fig. 7, A–C; and Fig. S3 E). We also tested the in vivo tumorigenicity in tumor xenograft experiments. Compared with control cells, MDA-MB231 cells with knockdown of AKR1B1 expression resulted in significantly reduced tumor growth (Fig. 7 D), whereas T47D cells with AKR1B1 expression caused dramatically enhanced tumor growth in vivo (Fig. 7 F). In addition, we examined the expression of AKR1B1, RelA, Twist2, and E-cadherin by Western blotting in tumor samples from a mouse model. Consistent with the analysis of cell lines, knockdown of AKR1B1 expression significantly caused an increase in E-cadherin expression and a decrease in RelA and Twist2 expression (Fig. S5 C), indicating that AKR1B1 regulates the EMT program by the same mechanism in vitro and in vivo. In line with these findings, mice given epalrestat exhibited substantially decreased tumor growth compared with control mice (Fig. S5 D). Then, we evaluated the effect of epalrestat treatment after tumor formation. Epalrestat was administered intragastrically 10 d after injection of MDA-MB-231 cells. Consistently, mice given

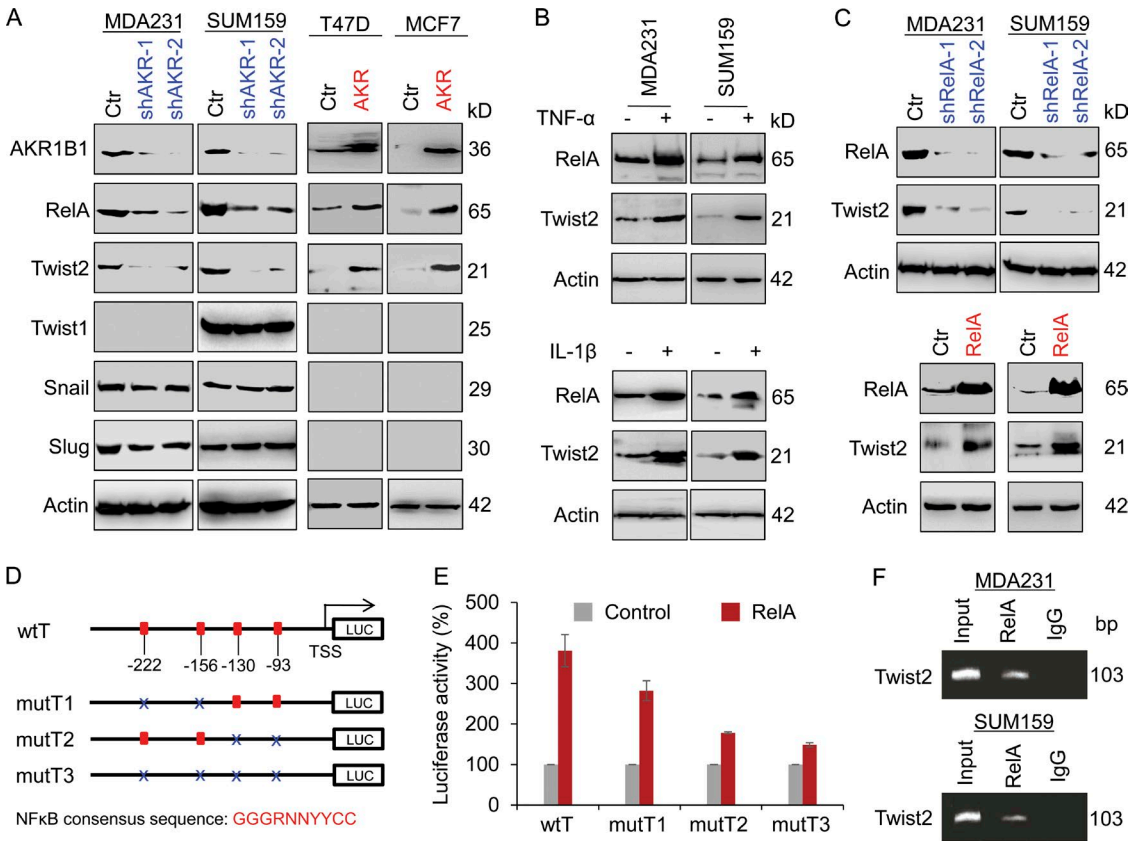

Figure 5. **RelA transcriptionally induces Twist2 expression.** (A) Expression of AKR1B1, RelA, Snail, Slug, Twist1, and Twist2 was analyzed by Western blotting in MDA-MB231 and SUM159 cells with stable empty vector (Ctr) or knockdown of AKR1B1 expression (left), as well as T47D and MCF7 cells with stable empty vector or AKR1B1 expression (right). (B) MDA-MB231 and SUM159 cells were treated with either 20 ng/ml TNF (top) or 20 ng/ml IL-1β (bottom) for 12 h, and expression of RelA and Twist2 was analyzed by Western blotting. (C) Expression of RelA and Twist2 was analyzed by Western blotting in MDA-MB231 and SUM159 cells with stable empty vector or knockdown of RelA expression (top), as well as cells with stable empty vector or RelA expression (bottom). (D) Schematic diagram showing positions of potential NF-κB–binding motifs in the Twist2 promoter. Twist2 promoter luciferase (LUC) construct and mutated derivatives are also shown. NF-κB consensus sequence: GGGRNNYYCC. R is purine, Y is pyrimidine, and N is any base. (E) Twist2 promoter luciferase construct (wtT) as well as its mutants (mutT1, mutT2, and mutT3) were coexpressed with empty vector or RelA in T47D cells. After 48 h, luciferase activities were determined and normalized. Data are mean ± SD in three separate experiments. (F) ChIP analysis for binding of RelA to the Twist2 promoter in MDA-MB231 and SUM159 cells.

epalrestat also exhibited significantly decreased tumor growth compared with control mice (Fig. 7 E). Next, we investigated whether inhibition of AKR1B1 expression affected tumor metastasis in a xenograft metastasis model in which MDA-MB231 cells were used to generate pulmonary metastases. Strikingly, knockdown of AKR1B1 expression or epalrestat greatly suppressed lung metastasis in vivo (Fig. 8, A and B). Collectively, these data suggest that AKR1B1 is critical for tumorigenicity and metastasis of BLBC cells, and pharmacologic inhibition of AKR1B1 can prevent tumorigenicity and metastasis of BLBC cells both in vitro and in vivo.

Having identified the critical function of AKR1B1 in breast cancer, we then sought to elucidate its clinical relevance by examining its correlation with patient survival in the NKI295 and GSE25066 datasets (van de Vijver et al., 2002; Hatzis et al., 2011). Patients were divided into two groups according to *AKR1B1* expression, with high *AKR1B1* expression having shorter survival in these patient cohorts (Fig. 8 C). Next, we evaluated whether *AKR1B1* expression was associated with the metastatic sites in a dataset (GEO accession no. GSE12276) that contains 204 breast cancer patients (Bos et al., 2009). Consistent with the metastatic tendency of BLBC, primary tumors with high *AKR1B1* expression preferentially metastasized to the brain and lungs (Fig. S5 E). These clinical validations strongly support the critical role of AKR1B1 in BLBC.

DISCUSSION

AKR1B1 facilitates the tumorigenic and metastatic capacity of BLBC cells through a positive regulatory feedback loop that activates the EMT program. Our study provides several mechanistic and therapeutic insights into the critical roles of AKR1B1 in EMT and BLBC.

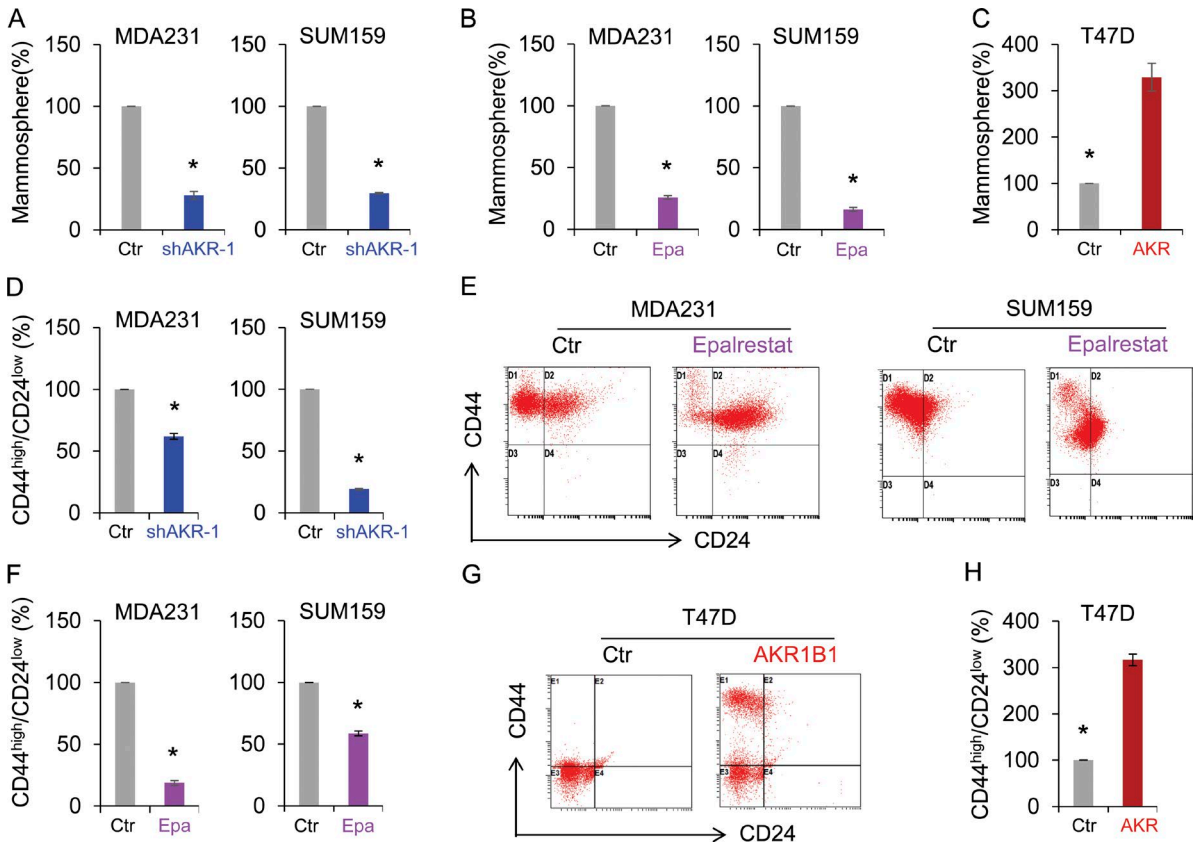

Figure 6. **AKR1B1 promotes tumorsphere formation and increases CSC population.** (A–C) Tumorsphere formation of MDA-MB231 and SUM159 cells with stable empty vector (Ctr) or knockdown of AKR1B1 expression (A) and MDA-MB231 and SUM159 cells treated with or without 20 µM epalrestat (Epa; B), as well as T47D cells with stable empty vector or AKR1B1 expression (C) was measured. Data are presented as a percentage of empty vector cell lines. *, $P < 0.01$ by Student's *t* test. (D–H) Populations of CSCs ($CD44^{high}/CD24^{low}$) were analyzed by flow cytometry in MDA-MB231 and SUM159 cells with stable empty vector or knockdown of AKR1B1 expression (D) and MDA-MB231 and SUM159 cells treated with or without 20 µM epalrestat (E and F), as well as T47D cells with stable empty vector or AKR1B1 expression (G and H). Representative images are shown in E and G. Data are presented as a percentage of empty vector cell lines. *, $P < 0.05$ by Student's *t* test. Data are mean ± SD in three separate experiments.

AKR1B1 regulates the EMT program through a positive feedback loop

The EMT program is a key event promoting carcinoma cell dissociation, invasion, and metastasis (Polyak and Weinberg, 2009; Ye and Weinberg, 2015). Loss of E-cadherin, which represents a hallmark of EMT, is often correlated with high tumor stage and metastasis (Thiery, 2009; Dong et al., 2013a). Several transcription factors, such as Snail, Twist1/2, and Zeb1/2, have been implicated in the transcriptional repression of E-cadherin and the induction of EMT (Yang et al., 2004; Kalluri and Weinberg, 2009; Thiery et al., 2009). Twist1 and Twist2 belong to highly conserved basic helix-loop-helix transcription factors that play pivotal roles in EMT and cancer metastasis (Šošić et al., 2003; Ansieau et al., 2010; Fang et al., 2011). Given the similarities of these two genes in sequence and function, a major unsolved question is whether Twist2 possesses the unique molecular targets and cellular functions. The findings that a frameshift mutation in the Twist2 gene causes Setleis syndrome and mutations in the Twist1 gene leads to Saethre-Chotzen syndrome exhibit different functions of two genes in bone and skin development (Chen and Behringer, 1995). In addition, the transcriptional expression pattern of Twist2 differs from that of Twist1 in various tumors (Ansieau et al., 2010). These observations suggest that both Twist2 and Twist1 have overlapping but distinct functions. Here, our finding revealed that Twist2 functions as a transcriptional activator to directly induce the transcription of AKR1B1 in contrast to Twist1, indicating that Twist2 has unique functions. Gene deletion experiments have shown that Twist2-knockout mice display disturbance of proinflammatory cytokines causing perinatal death (Šošić et al., 2003). However, the mechanism underlying the links between Twist2 and inflammation remains relatively unknown. Our data suggest that Twist2 may regulate inflammatory changes by direct transcriptional activation of AKR1B1 that has been implicated in the development of various inflammatory diseases and cancers.

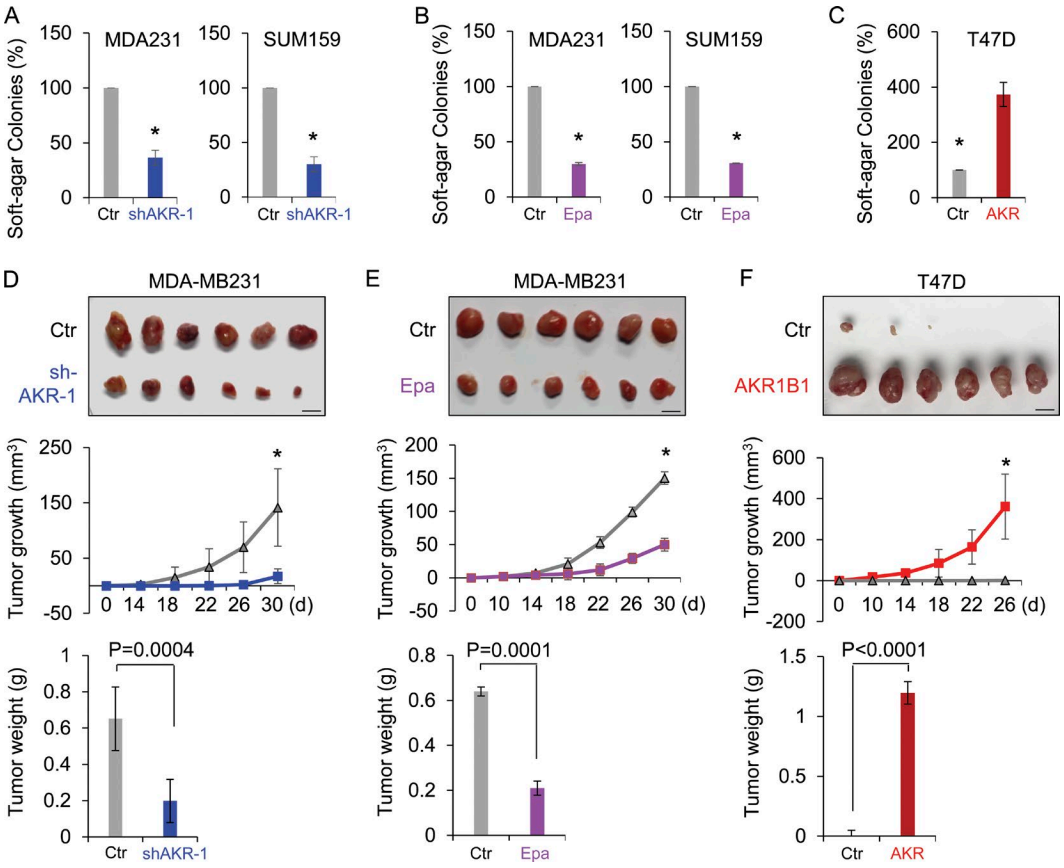

Figure 7. **AKR1B1 promotes tumorigenicity in vitro and in vivo.** (A–C) The formation of colonies from MDA-MB231 and SUM159 cells with stable empty vector (Ctr) or knockdown of AKR1B1 expression (A) and MDA-MB231 and SUM159 cells treated with or without 20 µM epalrestat (Epa; B), as well as T47D cells with stable empty vector or AKR1B1 expression (C) was measured. Data are presented as a percentage of empty vector cell lines and are mean ± SD in three separate experiments. *, $P < 0.01$ by Student's *t* test. (D–F) MDA-MB231 cells with stable empty vector or knockdown of AKR1B1 expression (D) as well as T47D cells with stable empty vector or AKR1B1 expression (F) were injected into the mammary fat pads of SCID mice. (E) For evaluation of epalrestat, after injection of MDA-MB231 cells on the left flank of every mouse, mice were divided into two groups (six mice per group). After 10 d, two groups of mice were intragastrically treated with 50 mg/kg/d epalrestat or sterile water, respectively. The growth of breast tumors was monitored every 2 d. Tumor size and weight were measured and recorded. Bars, 1 cm. Data are presented as mean ± SEM from six mice. *, $P < 0.001$.

It has been documented that AKR1B1 modulates NF-κB signaling via the PGF2a-mediated pathway (Ramana et al., 2004; Tammali et al., 2006). Consistent with this notion, AKR1B1 expression elevated PGF2a synthesis and RelA expression, indicating that AKR1B1 is critical part of a cellular program promoting PGF2a pathway flux, thus triggering NF-κB activation in BLBC. Activation of NF-κB is tightly associated with EMT induction (Huber et al., 2004; Zhou et al., 2004). Interestingly, we observed that only Twist2 expression was significantly up-regulated in cells with AKR1B1 overexpression, suggesting the involvement of AKR1B1 in Twist2 expression and EMT induction via the NF-κB signaling pathway. Indeed, our data identified that RelA is a transcriptional activator responsible for Twist2 expression, thus controlling the EMT program in BLBC.

Together, we demonstrate that AKR1B1 regulates the EMT program through a Twist2-mediated positive feedback regulatory loop. In BLBC cells, AKR1B1 expression is transcriptionally up-regulated by Twist2, leading to NF-κB activation via the PGF2a-mediated pathway. NF-κB, in turn, elevates Twist2 expression, which induces EMT, thus bridging AKR1B1 and the EMT program and fulfilling a positive feedback loop in BLBC (Fig. 8 D).

AKR1B1 enhances CSC properties and is required for tumorigenicity and metastasis in BLBC

BLBC is defined by expression of markers characteristic of basal/myoepithelial cells and identified as a subtype of breast cancer that may originate from undifferentiated stem cells (termed basal-like cells in the normal breast mammary gland; Polyak, 2011). Consistently, BLBC possesses more CSC and EMT characteristics than the other subtypes of breast cancer (Blick et al., 2008, 2010; Honeth et al., 2008; Sarrió et al., 2008; Storci et al., 2008; Bergamaschi et al., 2009; Hennessy et al., 2009). Elegant studies have showed that EMT is a cellular dedifferentiation program that confers tumor cells

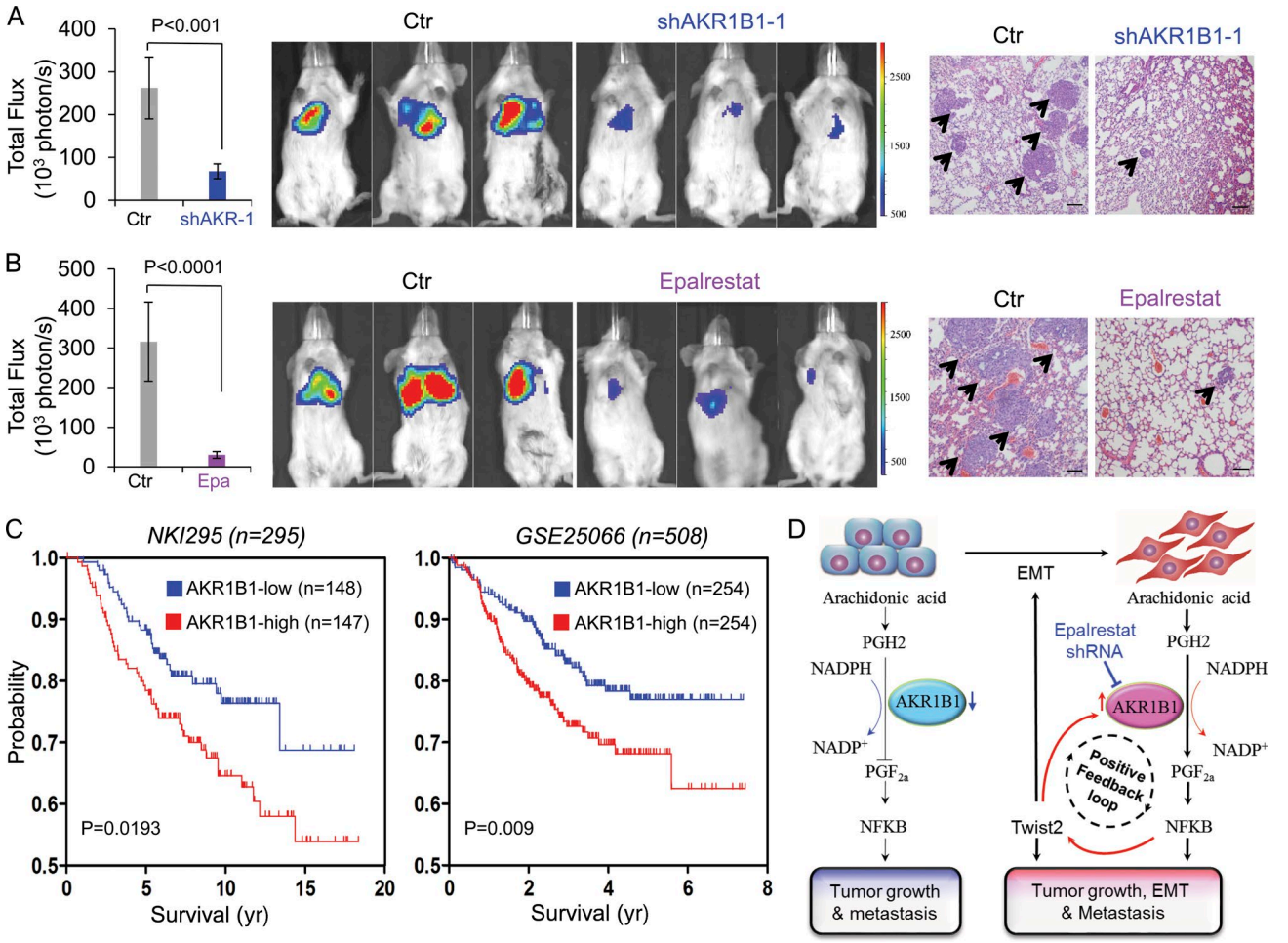

Figure 8. **AKR1B1 promotes metastasis in vivo.** (A and B) MDA-MB231 cells with stable empty vector (Ctr) or knockdown of AKR1B1 expression (A) as well as MDA-MB231 cells (B) were injected into SCID mice via the tail vein. For evaluation of epalrestat (Epa), the mice from B then received 50 mg/kg/d epalrestat or sterile water intragastrically. (Left) After 4 wk, the development of lung metastases was recorded using bioluminescence imaging and quantified by measuring photon flux (mean of six animals + SEM). (Middle) Three representative mice from each group are shown. (Right) Mice were also sacrificed. Lung metastatic nodules were examined in paraffin-embedded sections stained with hematoxylin and eosin. The arrowheads indicate lung metastases. Bars, 100 µm. (C) Kaplan-Meier survival analysis of published datasets (NKI295 and GSE25066) for the relationship between AKR1B1 expression and survival time. Differences were performed by the log-rank test. (D) A proposed model to illustrate the regulation of EMT by AKR1B1 through a positive feedback loop, leading to tumorigenicity and metastasis (see Discussion).

with CSC properties (Polyak and Weinberg, 2009; Thiery et al., 2009; Nauseef and Henry, 2011). In line with this notion, AKR1B1 expression leads to increased CSC properties by a positive feedback loop that activates the EMT program in BLBC, indicating that AKR1B1 is critical in controlling the viability of CSCs. Extensive studies have demonstrated that CSCs are essential for tumor initiation, recurrence, and metastasis (Rosen and Jordan, 2009; Liu and Wicha, 2010; Badve and Nakshatri, 2012). Indeed, our experiments showed that AKR1B1 expression in luminal cells increased tumorigenicity, whereas knockdown of AKR1B1 expression in BLBC cells suppressed tumorigenicity and metastasis in vitro and in vivo. Clinically, high AKR1B1 expression occurs specifically in BLBC and predicts poor relapse-free survival. Furthermore, AKR1B1 overexpression is also highly correlated with metastatic dissemination to the brain and lungs, which is completely in concordance with the metastatic propensity of BLBC. Clearly, our study suggests that AKR1B1 overexpression represents an oncogenic event that is responsible for the aggressive behaviors of BLBC cells.

AKR1B1 represents a potential therapeutic target for treating BLBC

The treatment of BLBC is an unmet medical need because of the absence of effective targeted therapies and poor response to standard chemotherapy. Therefore, identification of the relevant molecular targets in BLBC may facilitate the development of effective tailored therapies to improve

patient outcomes. Our study identified the crucial roles of AKR1B1 in EMT and BLBC and showed a tight correlation between AKR1B1 and Twist2 in breast cancer cells. Twist2, as a transcription factor, is difficult to target therapeutically because of the absence of a clear ligand-binding domain. As a downstream target of Twist2, AKR1B1 might be a potentially valuable target for therapeutics against this metastatic disease. Epalrestat is the only AKR1B1 inhibitor that has been approved in Japan for the targeted treatment of diabetic complications, which is easily absorbed by tissues and has minimum adverse effects (Hotta et al., 2006). Intriguingly, epalrestat significantly attenuated the viability of CSCs within breast cancer cell populations. This finding may be especially important because traditional therapies often leave behind the minority CSCs that regenerate tumors (Gupta et al., 2009). Thus, it is conceivable that epalrestat can suppress tumor progression. Indeed, epalrestat dramatically inhibited cancer cell migration and invasion in vitro and suppressed tumorigenicity and metastasis of BLBC cells in mice models, displaying potent efficacy against BLBC.

As the safety profiles of marketed drugs are generally known, drug repositioning has been regarded as an efficient approach to drug discovery and a way to identify new treatment for other diseases (Mizushima, 2011). Epalrestat is generally safe in clinical trials at oral dosages of 50–200 mg three times a day for the targeted treatment of diabetic complications, and the plasma epalrestat concentration of 12 μM is reached 1 h after a single oral dose of 50 mg (Uchida et al., 1995; Ito et al., 2009). Significantly, a clinically achievable dose of epalrestat exhibits apparent inhibitory effect on BLBC progression using cellular and mice models. Because epalrestat is already on the market without any major toxicity, our study provides proof of principle to suggest that epalrestat has the potential to become a valuable targeted drug in clinical treatment of BLBC.

MATERIALS AND METHODS

Plasmids, shRNA, and antibodies

AKR1B1 shRNA was purchased from MISSION shRNA (Sigma-Aldrich). Human AKR1B1 was amplified from a HeLa cDNA library and subcloned into pLenti6.3/V5. The pBABE-Twist2 expression plasmid was provided by G. Ouyang (Xiamen University, Xiamen, China).

Antibodies against AKR1B1 and β-actin were purchased from Sigma-Aldrich. Antibodies against Vimentin and Twist2 were from Neomarkers and Abnova, respectively. Antibodies for Snail and Slug were from Cell Signaling Technology. Antibody for IKBα and RelA was from Santa Cruz Biotechnology, Inc. N-cadherin and E-cadherin antibodies were from EMD Millipore and BD, respectively.

Cell culture

MDA-MB231, SUM159, and MCF7 cells were grown in DMEM/F12 supplemented with 10% FBS. T47D and ZR75 cells were grown in RPMI 1640 plus 10% FBS. SUM1315 cells were cultured in DMEM/F12 supplemented with 5% FBS, 5 μg/ml insulin, and 10 ng/ml epidermal growth factor. For establishing stable transfectants with AKR1B1 expression or knockdown of AKR1B1 expression, BLBC cells and luminal cells were transfected with pLenti6.3/V5-AKR1B1 and AKR1B1 shRNA, respectively. Stable clones were selected with 300 ng/ml puromycin for 4 wk.

Immunostaining and immunoblotting

Experiments were performed as described previously (Dong et al., 2013b). For immunofluorescent staining, cells were grown on chamber slides, fixed with 4% paraformaldehyde, and treated with primary antibodies. Secondary antibodies were Texas red–conjugated goat anti–mouse or FITC-conjugated goat anti–rabbit (Molecular Probes).

Quantitative real-time PCR

Total RNA was isolated using an RNeasy Mini kit (QIAGEN) according to the manufacturer's instructions. Specific quantitative real-time PCR experiments were performed using SYBR Green Power Master Mix following the manufacturer's protocol (Applied Biosystems).

Luciferase reporter assay

Luciferase reporter assay was performed as described previously (Dong et al., 2012). Cell extracts were prepared 48 h after transfection, and luciferase activity was determined by the Dual-Luciferase Reporter Assay system (Promega). All experiments were performed three times in triplicate.

ChIP

ChIP assays were performed as described previously (Lin et al., 2010; Dong et al., 2012). Two pairs of primers were used for ChIP assays: 5′-TGGAGTTCCCAATCTTGCAT-3′ and 5′-GATCACCCTAATTGGCAGGT-3′ for the AKR1B1 promoter and 5′-AAGACCCACACAGGTCGAG-3′ and 5′-GTTCTCTCTCTGGGCGTGA-3′ for the Twist2 promoter. The cells were prepared to perform ChIP assay with the Imprint ChIP kit (Sigma-Aldrich) according to the manufacturer's instructions as described recently (Dong et al., 2012).

Detection of PGF2a, NADPH, and ROS

The concentration of PGF2a was detected using commercially available enzyme-linked immunosorbent assay kits (Enzo Life Sciences). NADPH levels were tested by an NAD PH assay kit (BioVision). Cellular ROS level was measured by incubating cells with DCFH-DA (Jiancheng Bioengineering Institute) at manufacture-recommended concentration for 1 h before analysis in a spectrophotometer (SynergyMx M5 Microplate Reader; Molecular Devices).

Colony formation assay

Colony formation assay was performed using double-layer soft agar in 24-well plates with a top layer of 0.35% agar and a bottom layer of 0.7% agar. Cells were seeded into 24-well

plates in the desired medium and cultured at 37°C for 14–21 d, and the colonies were stained and counted.

Migration and invasion assays

Migration and invasion assays were performed in Boyden chambers as described previously (Dong et al., 2013a). The cancer cells were stained and counted with a microscope. All experiments were performed at least twice in triplicate. Statistical analysis was performed using Student's *t* test; a p-value of <0.05 was considered significant.

Mammosphere assay

Mammosphere assays were performed following the protocol previously described (Grimshaw et al., 2008) by plating single-cell suspensions into ultralow-attachment 6-well plates (Corning) in mammosphere culturing conditions and counting after 7–14 d.

Flow cytometry analysis

For the detection of the $CD44^{high}/CD24^{low}$ population, cells were incubated in a volume of 100 µl with 2 µl of each monoclonal antibody: CD44-PE/Cy7 and CD24-PE (eBioscience). Cells were treated on ice for 30 min and washed twice before analysis in the cytometer (Cytomic FC 500MCL; Beckman Coulter).

Tumorigenesis assay and lung metastasis model

Animal experiments were performed according to procedures approved by the Institutional Animal Care and Use Committee at Zhejiang University. To examine the effect of AKR1B1 on tumorigenesis, female SCID mice (6–8 wk old) were injected with 10^6 exogenous AKR1B1-expressing or knockdown cells on the left flank and vector control cells on the right flank. To evaluate the drug efficacy, 50 mg/kg/d epalrestat was administered intragastrically after injection of MDA-MB-231 cells on the left flank of every mouse, and sterile water was used as the vehicle control. Tumor formation was examined every 2–4 d for a 4-wk period. Tumors' size and weight were measured. To test the effect of AKR1B1 on tumor metastasis, female SCID mice were injected with MDA-MB-231 cells (10^6 cells/mouse) with stable empty vector or knockdown of AKR1B1 expression via tail vein (six mice per group). For evaluation of epalrestat, mice were injected with MDA-MB-231 cells (10^6 cells/mouse) via tail vein (six mice per group) and then received 50 mg/kg/d epalrestat or sterile water intragastrically. After 4 wk, lung metastasis was detected using an imagining system (IVIS-100; Xenogen). Mice were also sacrificed; lung metastatic nodules were detected in paraffin-embedded sections stained with hematoxylin and eosin. Data were analyzed using Student's *t* test; a p-value <0.05 was considered significant.

Statistical analysis

Results are expressed as mean + SD or SEM, as indicated. Comparisons were made using two-tailed Student's *t* test or one-way ANOVA. Correlations between AKR1B1 and Twist2 were analyzed using Pearson's correlation method and Spearman's rank correlation test. Survival curves were analyzed using the Kaplan-Meier method, and differences were performed with the log-rank test. In all statistical tests, $P < 0.05$ was considered statistically significant.

Online supplemental material

Fig. S1 shows AKR1B1 is up-regulated in BLBC. Fig. S2 shows AKR1B1 is a target of Twist2. Fig. S3 shows AKR1B1 is associated with migration, invasion, and colony formation of breast cancer cells. Fig. S4 shows AKR1B1-mediated NF-κB activation induces Twist2 expression. Fig. S5 shows silencing of AKR1B1 inhibits breast tumor growth and metastasis.

ACKNOWLEDGMENTS

Information about TCGA, the investigators, and institutions that constitute TCGA research network can be found at http://cancergenome.nih.gov/.

This work was supported by grants from the National Natural Science Foundation of China (81472455 to C. Dong and 81370730 and 81571512 to Q. Fu), the Key Program of the Natural Science Foundation of Zhejiang Province (LZ17H160002 to C. Dong), the Major Research Development Program of China (2016YFC1303200 to C. Dong), the Key Program of the Natural Science Foundation of Shandong Province (ZR2015JL027 to Q. Fu), Fundamental Research Funds for Central Universities of China (C. Dong), and the Thousand Young Talents Plan of China (C. Dong).

The authors declare no competing financial interests.

Author contributions: X. Wu, X. Li, Q. Fu, and C. Dong initiated the research, designed experiments, and analyzed data. X. Wu carried out the immunostaining, ChIP assay, colony formation assay, migration and invasion assays, enzyme-linked immunosorbent assay, and Western blot experiments. X. Li designed and conducted the tumorigenesis and lung metastasis experiments. Q. Fu performed the CSC-related work. Q. Cao and M. Wang generated most of the DNA constructs and performed the luciferase reporter assay. X. Chen performed the semiquantitative RT-PCR and quantitative real-time PCR. J. Yu and J. Yao performed the bioinformatic analysis. J. Long analyzed AKR1B1 expression in breast tumor tissues by Western blotting. H. Liu established stable clones with knockdown of RelA expression. D. Wang generated the Twist2 plasmids. R. Liao performed the ROS assay. C. Dong supervised the work and wrote the manuscript.

Submitted: 13 June 2016
Revised: 3 November 2016
Accepted: 20 December 2016

REFERENCES

Ansieau, S., A.P. Morel, G. Hinkal, J. Bastid, and A. Puisieux. 2010. TWI STing an embryonic transcription factor into an oncoprotein. *Oncogene.* 29:3173–3184. http://dx.doi.org/10.1038/onc.2010.92

Badve, S., and H. Nakshatri. 2012. Breast-cancer stem cells—beyond semantics. *Lancet Oncol.* 13:e43–e48. http://dx.doi.org/10.1016/S1470-2045(11)70191-7

Bergamaschi, A., G.O. Hjortland, T. Triulzi, T. Sørlie, H. Johnsen, A.H. Ree, H.G. Russnes, S. Tronnes, G.M. Maelandsmo, O. Fodstad, et al. 2009. Molecular profiling and characterization of luminal-like and basal-like in vivo breast cancer xenograft models. *Mol. Oncol.* 3:469–482. http://dx.doi.org/10.1016/j.molonc.2009.07.003

Blick, T., E. Widodo, H. Hugo, M. Waltham, M.E. Lenburg, R.M. Neve, and E.W. Thompson. 2008. Epithelial mesenchymal transition traits in human breast cancer cell lines. *Clin. Exp. Metastasis.* 25:629–642. http://dx.doi.org/10.1007/s10585-008-9170-6

Blick, T., H. Hugo, E. Widodo, M. Waltham, C. Pinto, S.A. Mani, R.A. Weinberg, R.M. Neve, M.E. Lenburg, and E.W. Thompson. 2010. Epithelial mesenchymal transition traits in human breast cancer cell lines parallel the $CD44^{hi/}CD24^{lo/-}$ stem cell phenotype in human breast cancer. *J. Mammary Gland Biol. Neoplasia.* 15:235–252. http://dx.doi.org/10.1007/s10911-010-9175-z

Bos, P.D., X.H. Zhang, C. Nadal, W. Shu, R.R. Gomis, D.X. Nguyen, A.J. Minn, M.J. van de Vijver, W.L. Gerald, J.A. Foekens, and J. Massagué. 2009. Genes that mediate breast cancer metastasis to the brain. *Nature.* 459:1005–1009. http://dx.doi.org/10.1038/nature08021

Brash, A.R. 2001. Arachidonic acid as a bioactive molecule. *J. Clin. Invest.* 107:1339–1345. http://dx.doi.org/10.1172/JCI13210

Carracedo, A., L.C. Cantley, and P.P. Pandolfi. 2013. Cancer metabolism: fatty acid oxidation in the limelight. *Nat. Rev. Cancer.* 13:227–232. http://dx.doi.org/10.1038/nrc3483

Chen, Z.F., and R.R. Behringer. 1995. Twist is required in head mesenchyme for cranial neural tube morphogenesis. *Genes Dev.* 9:686–699. http://dx.doi.org/10.1101/gad.9.6.686

D'Angio, C.T., and J.N. Finkelstein. 2000. Oxygen regulation of gene expression: a study in opposites. *Mol. Genet. Metab.* 71:371–380. http://dx.doi.org/10.1006/mgme.2000.3074

Dong, C., Y. Wu, J. Yao, Y. Wang, Y. Yu, P.G. Rychahou, B.M. Evers, and B.P. Zhou. 2012. G9a interacts with Snail and is critical for Snail-mediated E-cadherin repression in human breast cancer. *J. Clin. Invest.* 122:1469–1486. http://dx.doi.org/10.1172/JCI57349

Dong, C., Y. Wu, Y. Wang, C. Wang, T. Kang, P.G. Rychahou, Y.I. Chi, B.M. Evers, and B.P. Zhou. 2013a. Interaction with Suv39H1 is critical for Snail-mediated E-cadherin repression in breast cancer. *Oncogene.* 32:1351–1362. http://dx.doi.org/10.1038/onc.2012.169

Dong, C., T. Yuan, Y. Wu, Y. Wang, T.W. Fan, S. Miriyala, Y. Lin, J. Yao, J. Shi, T. Kang, et al. 2013b. Loss of FBP1 by Snail-mediated repression provides metabolic advantages in basal-like breast cancer. *Cancer Cell.* 23:316–331. http://dx.doi.org/10.1016/j.ccr.2013.01.022

Fang, X., Y. Cai, J. Liu, Z. Wang, Q. Wu, Z. Zhang, C.J. Yang, L. Yuan, and G. Ouyang. 2011. Twist2 contributes to breast cancer progression by promoting an epithelial–mesenchymal transition and cancer stem-like cell self-renewal. *Oncogene.* 30:4707–4720. http://dx.doi.org/10.1038/onc.2011.181

Fillmore, C., and C. Kuperwasser. 2007. Human breast cancer stem cell markers CD44 and CD24: enriching for cells with functional properties in mice or in man? *Breast Cancer Res.* 9:303. http://dx.doi.org/10.1186/bcr1673

Gloire, G., S. Legrand-Poels, and J. Piette. 2006. NF-κB activation by reactive oxygen species: fifteen years later. *Biochem. Pharmacol.* 72:1493–1505. http://dx.doi.org/10.1016/j.bcp.2006.04.011

Grimshaw, M.J., L. Cooper, K. Papazisis, J.A. Coleman, H.R. Bohnenkamp, L. Chiapero-Stanke, J. Taylor-Papadimitriou, and J.M. Burchell. 2008. Mammosphere culture of metastatic breast cancer cells enriches for tumorigenic breast cancer cells. *Breast Cancer Res.* 10:R52. http://dx.doi.org/10.1186/bcr2106

Gupta, P.B., T.T. Onder, G. Jiang, K. Tao, C. Kuperwasser, R.A. Weinberg, and E.S. Lander. 2009. Identification of selective inhibitors of cancer stem cells by high-throughput screening. *Cell.* 138:645–659. http://dx.doi.org/10.1016/j.cell.2009.06.034

Hanahan, D., and R.A. Weinberg. 2011. Hallmarks of cancer: the next generation. *Cell.* 144:646–674. http://dx.doi.org/10.1016/j.cell.2011.02.013

Hatzis, C., L. Pusztai, V. Valero, D.J. Booser, L. Esserman, A. Lluch, T. Vidaurre, F. Holmes, E. Souchon, H. Wang, et al. 2011. A genomic predictor of response and survival following taxane-anthracycline chemotherapy for invasive breast cancer. *JAMA.* 305:1873–1881. http://dx.doi.org/10.1001/jama.2011.593

Hennessy, B.T., A.M. Gonzalez-Angulo, K. Stemke-Hale, M.Z. Gilcrease, S. Krishnamurthy, J.S. Lee, J. Fridlyand, A. Sahin, R. Agarwal, C. Joy, et al. 2009. Characterization of a naturally occurring breast cancer subset enriched in epithelial-to-mesenchymal transition and stem cell characteristics. *Cancer Res.* 69:4116–4124. http://dx.doi.org/10.1158/0008-5472.CAN-08-3441

Hoeflich, K.P., C. O'Brien, Z. Boyd, G. Cavet, S. Guerrero, K. Jung, T. Januario, H. Savage, E. Punnoose, T. Truong, et al. 2009. In vivo antitumor activity of MEK and phosphatidylinositol 3-kinase inhibitors in basal-like breast cancer models. *Clin. Cancer Res.* 15:4649–4664. http://dx.doi.org/10.1158/1078-0432.CCR-09-0317

Honeth, G., P.O. Bendahl, M. Ringnér, L.H. Saal, S.K. Gruvberger-Saal, K. Lövgren, D. Grabau, M. Fernö, A. Borg, and C. Hegardt. 2008. The $CD44^{+}/CD24^{-}$ phenotype is enriched in basal-like breast tumors. *Breast Cancer Res.* 10:R53. http://dx.doi.org/10.1186/bcr2108

Hotta, N., Y. Akanuma, R. Kawamori, K. Matsuoka, Y. Oka, M. Shichiri, T. Toyota, M. Nakashima, I. Yoshimura, N. Sakamoto, and Y. Shigeta. 2006. Long-term clinical effects of epalrestat, an aldose reductase inhibitor, on diabetic peripheral neuropathy: the 3-year, multicenter, comparative aldose reductase inhibitor-diabetes complications trial. *Diabetes Care.* 29:1538–1544. http://dx.doi.org/10.2337/dc05-2370

Huber, M.A., N. Azoitei, B. Baumann, S. Grünert, A. Sommer, H. Pehamberger, N. Kraut, H. Beug, and T. Wirth. 2004. NF-κB is essential for epithelial-mesenchymal transition and metastasis in a model of breast cancer progression. *J. Clin. Invest.* 114:569–581. http://dx.doi.org/10.1172/JCI200421358

Ito, A., R. Ishii-Nozawa, C. Ibuki, H. Atarashi, H. Kataoka, and K. Takeuchi. 2009. Examination of questionnaires regarding diabetic peripheral neuropathy in epalrestat-treated patients and their usefulness in the treatment of this disorder—influence on treatment course. *Yakugaku Zasshi.* 129:1239–1247. http://dx.doi.org/10.1248/yakushi.129.1239

Kalluri, R., and R.A. Weinberg. 2009. The basics of epithelial-mesenchymal transition. *J. Clin. Invest.* 119:1420–1428. http://dx.doi.org/10.1172/JCI39104

Kinoshita, J.H., P. Kador, and M. Catiles. 1981. Aldose reductase in diabetic cataracts. *JAMA.* 246:257–261. http://dx.doi.org/10.1001/jama.1981.03320030049032

Kreike, B., M. van Kouwenhove, H. Horlings, B. Weigelt, H. Peterse, H. Bartelink, and M.J. van de Vijver. 2007. Gene expression profiling and histopathological characterization of triple-negative/basal-like breast carcinomas. *Breast Cancer Res.* 9:R65. http://dx.doi.org/10.1186/bcr1771

Li, N., and M. Karin. 1999. Is NF-κB the sensor of oxidative stress? *FASEB J.* 13:1137–1143.

Lin, Y., Y. Wu, J. Li, C. Dong, X. Ye, Y.I. Chi, B.M. Evers, and B.P. Zhou. 2010. The SNAG domain of Snail1 functions as a molecular hook for recruiting lysine-specific demethylase 1. *EMBO J.* 29:1803–1816. http://dx.doi.org/10.1038/emboj.2010.63

Liu, S., and M.S. Wicha. 2010. Targeting breast cancer stem cells. *J. Clin. Oncol.* 28:4006–4012. http://dx.doi.org/10.1200/JCO.2009.27.5388

Liu, H.X., X.L. Li, and C.F. Dong. 2015. Epigenetic and metabolic regulation of breast cancer stem cells. *J. Zhejiang Univ. Sci. B.* 16:10–17. http://dx.doi.org/10.1631/jzus.B1400172

Mani, S.A., W. Guo, M.J. Liao, E.N. Eaton, A. Ayyanan, A.Y. Zhou, M. Brooks, F. Reinhard, C.C. Zhang, M. Shipitsin, et al. 2008. The epithelial-mesenchymal transition generates cells with properties of stem cells. *Cell.* 133:704–715. http://dx.doi.org/10.1016/j.cell.2008.03.027

Mizushima, T. 2011. Drug discovery and development focusing on existing medicines: drug re-profiling strategy. *J. Biochem.* 149:499–505. http://dx.doi.org/10.1093/jb/mvr032

Nauseef, J.T., and M.D. Henry. 2011. Epithelial-to-mesenchymal transition in prostate cancer: paradigm or puzzle? *Nat. Rev. Urol.* 8:428–439. http://dx.doi.org/10.1038/nrurol.2011.85

Neve, R.M., K. Chin, J. Fridlyand, J. Yeh, F.L. Baehner, T. Fevr, L. Clark, N. Bayani, J.P. Coppe, F. Tong, et al. 2006. A collection of breast cancer cell lines for the study of functionally distinct cancer subtypes. *Cancer Cell.* 10:515–527. http://dx.doi.org/10.1016/j.ccr.2006.10.008

Onder, T.T., P.B. Gupta, S.A. Mani, J. Yang, E.S. Lander, and R.A. Weinberg. 2008. Loss of E-cadherin promotes metastasis via multiple downstream transcriptional pathways. *Cancer Res.* 68:3645–3654. http://dx.doi.org/10.1158/0008-5472.CAN-07-2938

Polyak, K. 2011. Heterogeneity in breast cancer. *J. Clin. Invest.* 121:3786–3788. http://dx.doi.org/10.1172/JCI60534

Polyak, K., and R.A. Weinberg. 2009. Transitions between epithelial and mesenchymal states: acquisition of malignant and stem cell traits. *Nat. Rev. Cancer.* 9:265–273. http://dx.doi.org/10.1038/nrc2620

Rakha, E.A., J.S. Reis-Filho, and I.O. Ellis. 2008. Basal-like breast cancer: a critical review. *J. Clin. Oncol.* 26:2568–2581. http://dx.doi.org/10.1200/JCO.2007.13.1748

Ramana, K.V., B. Friedrich, S. Srivastava, A. Bhatnagar, and S.K. Srivastava. 2004. Activation of nuclear factor-κB by hyperglycemia in vascular smooth muscle cells is regulated by aldose reductase. *Diabetes.* 53:2910–2920. http://dx.doi.org/10.2337/diabetes.53.11.2910

Riaz, M., F. Elstrodt, A. Hollestelle, A. Dehghan, J.G. Klijn, and M. Schutte. 2009. Low-risk susceptibility alleles in 40 human breast cancer cell lines. *BMC Cancer.* 9:236. http://dx.doi.org/10.1186/1471-2407-9-236

Rosen, J.M., and C.T. Jordan. 2009. The increasing complexity of the cancer stem cell paradigm. *Science.* 324:1670–1673. http://dx.doi.org/10.1126/science.1171837

Sales, K.J., S.C. Boddy, and H.N. Jabbour. 2008. F-prostanoid receptor alters adhesion, morphology and migration of endometrial adenocarcinoma cells. *Oncogene.* 27:2466–2477. http://dx.doi.org/10.1038/sj.onc.1210883

Sarrió, D., S.M. Rodriguez-Pinilla, D. Hardisson, A. Cano, G. Moreno-Bueno, and J. Palacios. 2008. Epithelial-mesenchymal transition in breast cancer relates to the basal-like phenotype. *Cancer Res.* 68:989–997. http://dx.doi.org/10.1158/0008-5472.CAN-07-2017

Šošić, D., J.A. Richardson, K. Yu, D.M. Ornitz, and E.N. Olson. 2003. Twist regulates cytokine gene expression through a negative feedback loop that represses NF-κB activity. *Cell.* 112:169–180. http://dx.doi.org/10.1016/S0092-8674(03)00002-3

Srivastava, S.K., K.V. Ramana, and A. Bhatnagar. 2005. Role of aldose reductase and oxidative damage in diabetes and the consequent potential for therapeutic options. *Endocr. Rev.* 26:380–392. http://dx.doi.org/10.1210/er.2004-0028

Storci, G., P. Sansone, D. Trere, S. Tavolari, M. Taffurelli, C. Ceccarelli, T. Guarnieri, P. Paterini, M. Pariali, L. Montanaro, et al. 2008. The basal-like breast carcinoma phenotype is regulated by *SLUG* gene expression. *J. Pathol.* 214:25–37. http://dx.doi.org/10.1002/path.2254

Tammali, R., K.V. Ramana, S.S. Singhal, S. Awasthi, and S.K. Srivastava. 2006. Aldose reductase regulates growth factor-induced cyclooxygenase-2 expression and prostaglandin E2 production in human colon cancer cells. *Cancer Res.* 66:9705–9713. http://dx.doi.org/10.1158/0008-5472.CAN-06-2105

Tammali, R., S.K. Srivastava, and K.V. Ramana. 2011. Targeting aldose reductase for the treatment of cancer. *Curr. Cancer Drug Targets.* 11:560–571. http://dx.doi.org/10.2174/156800911795655958

Thiery, J.P. 2009. [Epithelial-mesenchymal transitions in cancer onset and progression]. *Bull. Acad Natl. Med.* 193:1969–1979.

Thiery, J.P., H. Acloque, R.Y. Huang, and M.A. Nieto. 2009. Epithelial-mesenchymal transitions in development and disease. *Cell.* 139:871–890. http://dx.doi.org/10.1016/j.cell.2009.11.007

Uchida, K., T. Kigoshi, S. Nakano, T. Ishii, M. Kitazawa, and S. Morimoto. 1995. Effect of 24 weeks of treatment with epalrestat, an aldose reductase inhibitor, on peripheral neuropathy in patients with non-insulin-dependent diabetes mellitus. *Clin. Ther.* 17:460–466. http://dx.doi.org/10.1016/0149-2918(95)80111-1

Valastyan, S., and R.A. Weinberg. 2011. Tumor metastasis: molecular insights and evolving paradigms. *Cell.* 147:275–292. http://dx.doi.org/10.1016/j.cell.2011.09.024

van de Vijver, M.J., Y.D. He, L.J. van't Veer, H. Dai, A.A. Hart, D.W. Voskuil, G.J. Schreiber, J.L. Peterse, C. Roberts, M.J. Marton, et al. 2002. A gene-expression signature as a predictor of survival in breast cancer. *N. Engl. J. Med.* 347:1999–2009. http://dx.doi.org/10.1056/NEJMoa021967

Vargo-Gogola, T., and J.M. Rosen. 2007. Modelling breast cancer: one size does not fit all. *Nat. Rev. Cancer.* 7:659–672. http://dx.doi.org/10.1038/nrc2193

Yang, J., S.A. Mani, J.L. Donaher, S. Ramaswamy, R.A. Itzykson, C. Come, P. Savagner, I. Gitelman, A. Richardson, and R.A. Weinberg. 2004. Twist, a master regulator of morphogenesis, plays an essential role in tumor metastasis. *Cell.* 117:927–939. http://dx.doi.org/10.1016/j.cell.2004.06.006

Ye, X., and R.A. Weinberg. 2015. Epithelial–mesenchymal plasticity: A central regulator of cancer progression. *Trends Cell Biol.* 25:675–686. http://dx.doi.org/10.1016/j.tcb.2015.07.012

Zhou, B.P., J. Deng, W. Xia, J. Xu, Y.M. Li, M. Gunduz, and M.C. Hung. 2004. Dual regulation of Snail by GSK-3β-mediated phosphorylation in control of epithelial–mesenchymal transition. *Nat. Cell Biol.* 6:931–940. http://dx.doi.org/10.1038/ncb1173